Progress In Electromagnetics Research, PIER 70, 269–280, 2007

LOWPASS FILTER DESIGN OF HILBERT CURVE RING DEFECTED GROUND STRUCTURE

J. Chen, Z.-B. Weng, Y.-C. Jiao, and F.-S. Zhang

National Key Laboratory of Antennas and Microwave Technology
Xidian University
Xi'an 710071, China

Abstract—In this paper, a novel Hilbert curve ring (HCR) fractal defected ground structure (DGS) and its equivalent circuit are investigated. Furthermore, an improved HCR DGS cell model with open stubs loaded on the conductor line is then presented to improve the out-band suppression. By employing three cascaded improved HCR DGS cells, an L-band microstrip low-pass is designed and fabricated. This lowpass filter achieves a quite steep rejection property; a low in-band insertion loss of below 0.5 dB and a high out-band suppression of more than 33 dB.

1. INTRODUCTION

Recently, there has been an increasing interest in the applications of defected ground structure (DGS) in microwave and millimeter-wave applications [1–3]. The DGS of the microstrip line employs an intentional defect on the ground and it provides band rejection characteristic from the resonance property. The applications of the DGS are developed in divider, filter, and amplifier circuits. The defect of the conventional DGS is with the dumbbell shape or the rectangle shape, these conventional DGSs, however, have a flat slope of their rejection characteristic. To fabricate a lowpass filter with steep rejection property, many these DGSs are needed to be cascaded, which also means higher in-band insertion and larger size.

Different from Euclidean geometries, fractal geometries have two common properties, space-filling and self-similarity. It has been shown that the self-similarity property of fractal shapes can be successfully applied to the design of multi-band fractal antennas, such as the Sierpinski gasket antenna [4], while the space-filling property of fractals can be utilized to reduce antenna size [5, 6].

In this paper, a novel Hilbert curve ring (HCR) DGS is proposed to design a lowpass filter with steep rejection property, and its equivalent circuit is studied. This DGS structure has a flat low-pass characteristic and a sharp band-gap property compared to the conventional dumbbell DGS. An analysis of the relationship between the transmission characteristic and the HCR dimension is made. In order to enhance the out-band suppression, an improved HCR DGS cell model loaded with open-stubs is proposed. Based on the improved modal, a compact L-band microstrip low-pass filter with periodic HCR DGS is designed and fabricated. Both the simulation and measurement results show that the filter has steep rejection property, perfect low-pass characteristic and high out-band suppression.

2. CONFIGURATION AND CHARACTERISTIC OF HCR DGS

2.1. Configuration of the HCR DGS Cell

Since novel, Hilbert curve is introduced at first. Various iteration stages of Hilbert curves are shown in Fig. 1, it may be observed that geometry at a stage can be obtained by putting together four copies of the previous iteration, connected with additional line segments. For example, the geometry of order 3 can be thought of as four copies of the geometry with order 2 (arranged in different orientations), connected with the additional segments shown by broken lines.

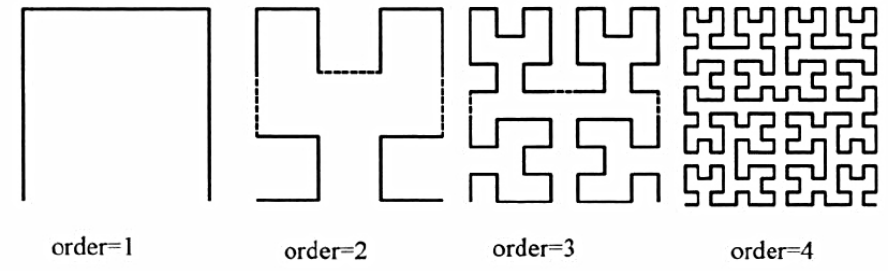

Figure 1. First four fractal iterations for the Hilbert curve geometry.

HCR DGS is obtained by etching a split-ring [7], of which, the inner edge is a modified 3 order Hilbert curve, and the outer edge is a rectangle, as shown in Fig. 2. The orientation of the split-gap will have distinct influence on the transmission property, if the orientation is rotated by 90 degrees, the slop of its rejection characteristic became flat just like that of dumbbell DGS, so it is chosen perpendicularly

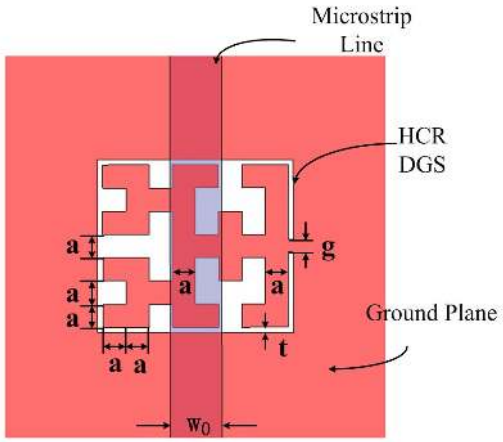

Figure 2. HCR DGS cell model.

to the conductor line for our purpose. The permittivity of the microstrip line is $\varepsilon_r = 2.65$, the height of the dielectric board is $h = 1.5\,\text{mm}$ and width of the conductor line is 4.1 mm, witch is chosen for the characteristic impedance of 50-ohm microstrip line. Due to the discontinuity of impedance in defective region, an electromagnetic resonance is obtained and thus band-gaps are formed.

2.2. Characteristic and Equivalent circuit of HCR DGS

An example HCR DGS unit with segment-length of Hilbert curve $a = 1.2\,\text{mm}$, split-gap $g = 1\,\text{mm}$, and ring-width $t = 0.4\,\text{mm}$ is simulated by EM simulator Ansoft HFSS 10. Fig. 3 shows the simulation results. It can be observed that unlike dumbbell DGS, the proposed DGS have 3 attenuation poles. The insertion of pass-band below the first attenuation pole is low and the rejection property is quite steep, which is suitable to be as the basic unit of a low-pass filter. However, this structure has the disadvantages such as narrow bandwidth of band-gap and insufficient suppression in high frequency range.

The sensitivity of filters is defined as [8]:

$$\xi = \frac{\alpha_{\min} - \alpha_{\max}}{f_s - f_c}$$

where, ξ = sensitivity in dB/GHz, $\alpha_{\max}$ = the 3 dB attenuation point, $\alpha_{\min}$ = 20 dB attenuation point, f_s = 20 dB stopband frequency, f_c = 3 dB cutoff frequency.

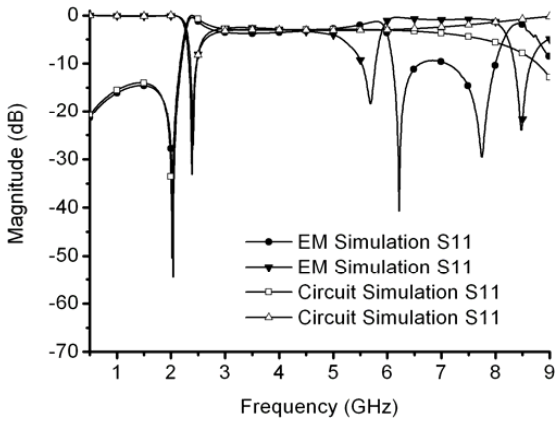

Figure 3. Simulation results for the proposed DGS unit. ($a = 1.2$mm, $t = 0.4$ mm, $g = 1$ mm)

Table 1 shows HCR DGS have much higher sensitivity than other DGSs, which also means that HCR DGS has much steeper rejection property.

Table 1. Sensitivity of different DGSs.

	Dumbbell [2]	Double Equilateral U-Shaped [10]	Split-ring Resonator [9]	Proposed
f_c (GHz)	3.62	2.10	3.14	2.30
f_0 (GHz)	4.88	2.60	3.80	2.41
f_s (GHz)	4.70	2.50	3.70	2.39
$f_s - f_c$ (GHz)	1.08	0.40	0.56	0.09
ξ (dB/GHz)	15.7	42.5	30.35	188.9

Because the characteristic of low pass filter which the author interests in mainly depend on the first attenuation pole, the equivalent circuit [9] shown in Fig. 4 will only consider the first attenuation pole. The equivalent circuit of a 50-ohm transmission line is composed of two serial inductors and a shunt capacitor, and the Hilbert curve ring forms a parallel resonator. Therefore, etching Hilbert curve ring defective pattern in the ground plane will add a parallel resonator to the equivalent circuit of the 50-ohm transmission line, but will have

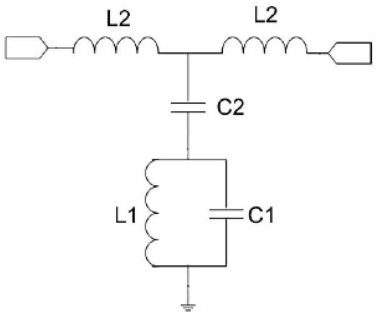

Figure 4. Equivalent circuit of the proposed DGS unit.

a little affection on the value of the elements L_2 and C_2. The first attenuation pole for the HCR DGS cell is determined by the resonant frequency of the shunt circuit, that means it is codetermined by L_1, C_1 and C_2.

The impedance of the parallel LC circuit is given by

$$Z_1 = \frac{1}{j\omega C_1 + \frac{1}{j\omega L_1}} = j\frac{\omega L_1}{1 - \omega^2 L_1 C_1} \tag{1}$$

While the impedance of the single capacitor C_2 is

$$Z_2 = \frac{1}{j\omega C_2} = -j\frac{1}{\omega C_2} \tag{2}$$

The attenuation pole is obtained when

$$Z_1 + Z_2 = 0 \tag{3}$$

Then we have the resonant frequency as

$$f_s = \frac{1}{2\pi\sqrt{L_1(C_1 + C_2)}} \tag{4}$$

As shown in Fig. 3, the circuit simulation and EM simulation agree well with each other at the first attenuation pole.

The authors investigate the dependence of the transmission characteristic on segment-length of Hilbert curve a, ring-width of HCR t. The line-width is chosen to be the characteristic impedance of 50-ohm microstrip line, split-gap g is kept constant to 1 mm, and the substrate with 1.5mm thickness and a dielectric constant of 2.65 is used for all simulations. Two HCR DGS unit circuits without any

period are simulated with the different dimension, there is only one parameter varying for each case.

In case one, ring-width t is 0.4 mm. As the segment-length of Hilbert curve a is increased, the cutoff frequency reduced and all of the three attenuation pole locations move to lower frequency, as seen in Fig. 5(a).

Then in case two, the segment-length of Hilbert curve a is kept constant to 1.2 mm, while the ring-width t varies. The simulation

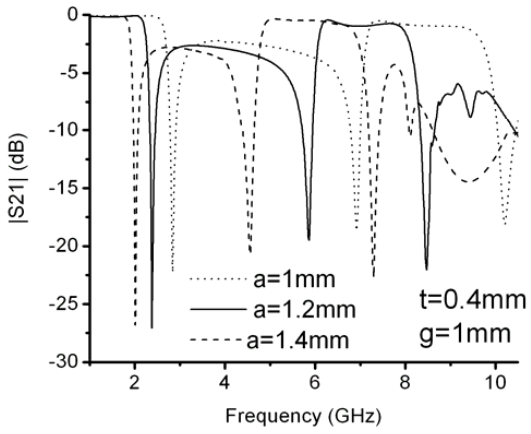

(a)

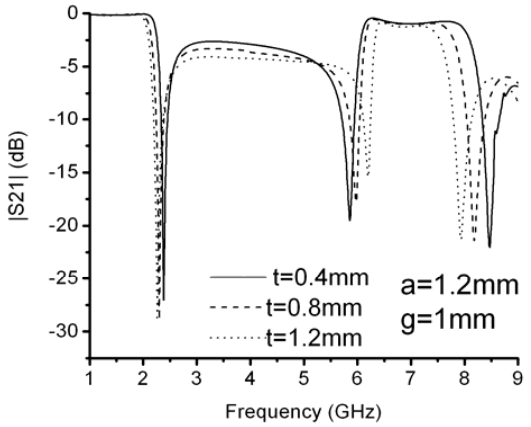

(b)

Figure 5. Variation of transmission curve with segment-length of Hilbert curve a (a) and ring-width t (b).

results are shown in Fig. 5(b). As t increase, the first attenuation pole relocated at a litter lower frequency, the second attenuation pole location move to higher frequency, while the third attenuation pole location shift to lower frequency.

3. CONFIGURATION AND CHARACTERISTIC OF THE IMPROVED HCR DGS CELL

To suppress the out-band suppression, open stubs on the conductor line are loaded, here, open stubs act as parallel capacitors. The topology and the equivalent circuit of the HCR DGS cell with open stubs are depicted in Fig. 6 and Fig. 7, respectively. For all cases, microstrip line composed of teflon substrate with thickness $h = 1.5\,\text{mm}$ and dielectric constant $\varepsilon_r = 2.65$ is considered, the conductor line has a width of $w_0 = 4.1\,\text{cm}$. The HCR DGS cell has a segment-length of Hilbert curve of $a = 1.2\,\text{mm}$, a split-gap of $g = 1\,\text{mm}$, and ring-width of $t = 0.4\,\text{mm}$.

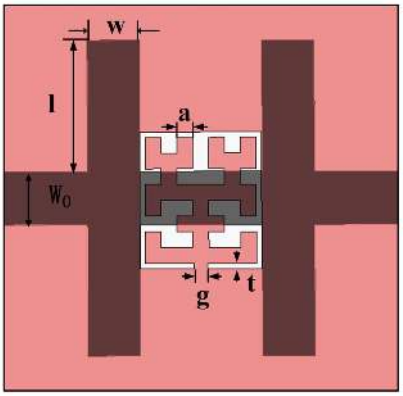

Figure 6. Layout of the improved HCR DGS cell.

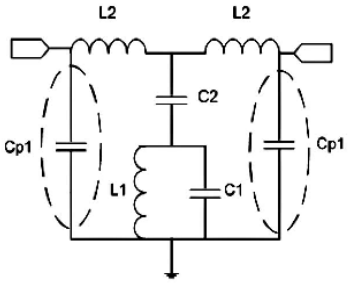

Figure 7. Equivalent circuit of the improved HCR DGS.

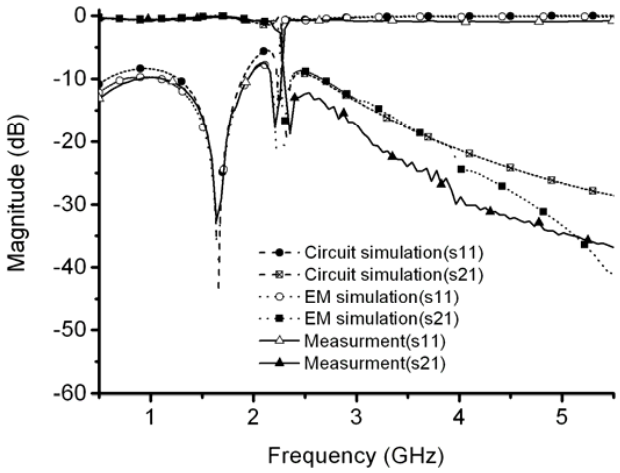

Figure 8. Simulation and measurement results for the improved HCR DGS.

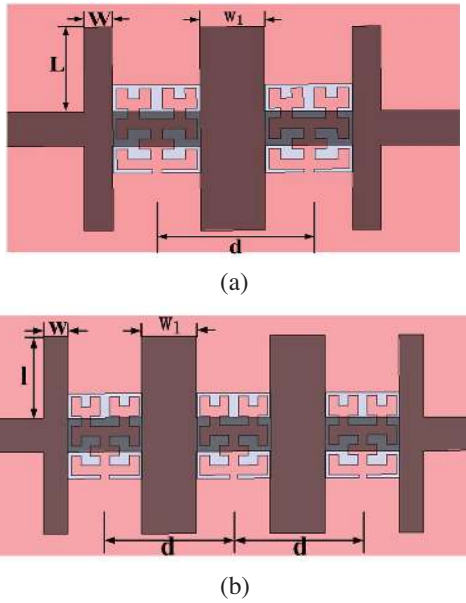

Figure 9. Layout of the HCR DGS lowpass filter. (a) 2-cell, (b) 3-cell.

Table 2. Equivalent circuit values with the number of HCR DGS cells.

Cell Number	**1 (no stub)**	**1 (with stub)**	**2**	**3**
L_1/nH	4.46	4.46	4.46	4.46
L_2/nH	2.187	2.187	2.187	2.187
C_1/pF	0.441	0.441	0.441	0.441
C_2/pF	0.557	0.557	0.557	0.557
Cp_1/pF	-	2.78	2.43	1.85
Cp_2/pF	-	-	4.36	3.28
Cutoff frequency f_c/GHz	2.25	2.25	2.25	2.25
Edge suppression L_s/dB	-27.1	-18.7	-31.3	-51.2

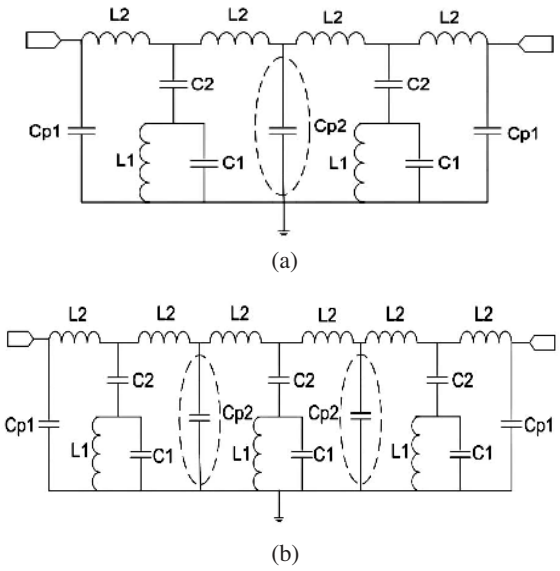

Figure 10. Equivalent circuit of the HCR DGS lowpass filters. (a) 2-cell, (b) 3-cell.

For the improved HCR DGS cell, all the open stubs placed on the conductor line have a width of $w = 4\,\text{mm}$ and length of $10\,\text{mm}$.

As shown in Fig. 8, the suppression in out-band for the proposed configuration is much larger than that without stubs, and the simulated result and measurement agree well with each other.

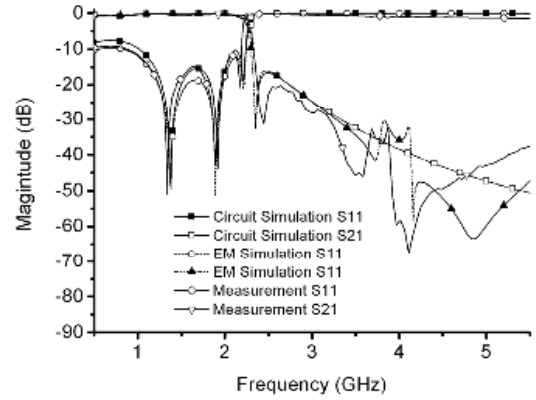

(a)

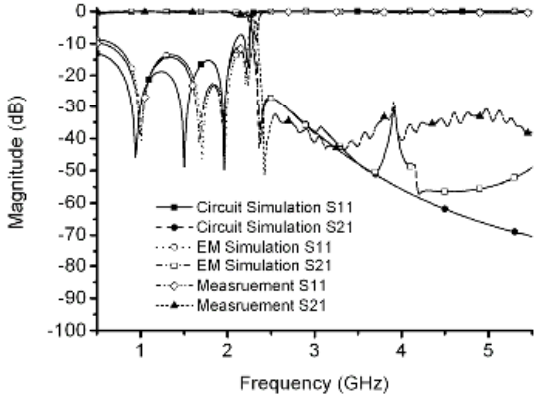

(b)

Figure 11. Simulation and measurement results for the HCR DGS lowpass filter. (a) 2-cell, (b) 3-cell.

4. LOWPASS FILTER DESIGN AND MEASUREMENT RESULTS

In order to demonstrate the effectiveness of this improved DGS unit, two lowpass filters are designed and fabricated. Fig. 9 illustrates the topology of these two filters, Fig. 10 shows the equivalent circuit of these two filters, Fig. 11 reports both simulation and measurement results for them, and Fig. 12 depicts photographs of the proposed

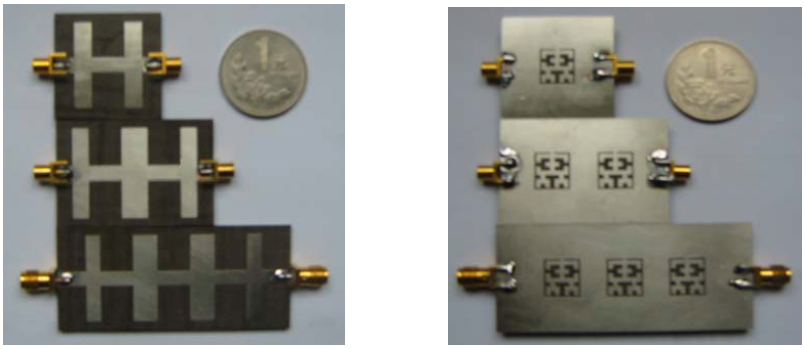

(a) (b)

Figure 12. Photograph of fabricated HCR DGS with different cell numbers. (a) top view, (b) bottom View.

filters with different cell numbers. For the 2-cell HCR DGS filter, the dimensions of the stubs are $l = 10\,\text{mm}$, $w = 3\,\text{mm}$, $w_1 = 6.8\,\text{mm}$ and the distance d is correspond fixed as 16 mm. For the 3-cell one, the dimension of the stubs are set as $l = 9.9\,\text{mm}$, $w = 3\,\text{mm}$, $w_1 = 6.8\,\text{mm}$, and distance d is given as 16 mm. The equivalent circuit values are optimized and extracted, as shown in Table 2. From the Fig. 11, it can be seen that this two filters have a good lowpass property, the cut-off frequency and the attenuation pole location have been found to be $f_c = 2.25\,\text{GHz}$ and $f_0 = 2.4\,\text{GHz}$, respectively. Measured passband loss is below 0.5 dB, a sharp slop and high suppression are obtained at band edge. In a wide frequency range, the out-band suppression is almost less than 20 dB for 2-cell filter and 33 dB for 3-cell filter, respectively.

5. CONCLUSION

A novel Hilbert curve ring (HCR) DGS is proposed and analyzed in detail. Compared with the conventional dumbbell DGS cell, this structure has a flat fluctuation in low frequency range and a sharp slop at edge frequency. The out-band suppression of the HCR DGS cell can be improved by placing open-stubs on the conductor line, based on the improved cell, compact lowpass filter is designed and fabricated, which has a very sharp slop, low in-band loss, and high suppression of appropriate 33 dB within a wide out-band frequency range.

REFERENCES

1. Lim, J. S., Y. C. Jeong, D. Ahn, and S. Nam, "A technique reducing the size of microwave amplifiers using spiral-shaped defected ground structure," *J. Korea Electromag. Eng.*, Vol. 14, No. 9, 904–911, Sept. 2003.
2. Kim, C. S., J. S. Park, and D. Ahn, "A novel 1-D periodic defected ground structure for planar circuits," *IEEE Microwave Guided Wave Lett.*, Vol. 10, No. 4, 131–133, April 2000.
3. Sharma, R., T. Chakravarty, S. Bhooshan, and A. B. Bhattacharyya, "Design of a novel 3 db microstrip backward wave coupler using defected ground structure," *Progress In Electromagnetics Research*, PIER 65, 261–273, 2006.
4. Puente, C., J. Ponmeu, R. Pous, and A. Cardama, "On the behavior of the Sierpinski multiband antenna," *IEEE Transactions on Antennas and Propagation*, Vol. 46, No. 4, 517–524, April 1998.
5. Puente, C., J. Romeu, R. Pous, J. Ramis, and A. Hijazo, "Small but long Koch fractal monopole," *IEEE Electronics Letters*, Vol. 34, No. 1, 9–10, January 1998.
6. Yousefzadeh, N., C. Ghobadi, and M. Kamyab, "Consideration of mutual coupling in a microstrip patch array using fractal elements," *Progress In Electromagnetics Research*, PIER 66, 41–49, 2006.
7. Yao, H. Y., L. W. Li, Q. Wu, et al., "Macroscopic performance analysis of metamaterials synthesized from macroscopic 2-D isotropic cross split-ring resonator array," *Progress In Electronmagnetics Research*, PIER 51, 197–217, 2005.
8. Karmaker, N. C., "Improved performance of photonic band-gap microstrip line structures with the use of chebyshev distributions," *Microwave Opt. Tech. Lett.*, Vol. 33, No. 2002, 1–5, 2002.
9. Wu, B., B. Li, T. Su, and C.-H. Liang, "Equivalent circuit analysis and lowpass filter design of split-ring resonator DGS," *Journal of Electromagnetic Waves and Application*, Vol. 20, No. 14, 1943–1953, 2006.
10. Ting, S. W., K. W. Tam, and R. P. Martins, "Miniaturized microstrip lowpass filter with wide stopband using double equilateral U-shaped defected ground structure," *IEEE Microwave and Wireless Components Letters*, Vol. 16, No. 5, 240–242, May 2006.